



CHORUS

This is the accepted manuscript made available via CHORUS. The article has been published as:

Electron-Nuclear Energy Sharing in Above-Threshold Multiphoton Dissociative Ionization of H₂

J. Wu, M. Kunitski, M. Pitzer, F. Trinter, L. Ph. H. Schmidt, T. Jahnke, M. Magrakvelidze, C. B. Madsen, L. B. Madsen, U. Thumm, and R. Dörner

Phys. Rev. Lett. **111**, 023002 — Published 9 July 2013

DOI: [10.1103/PhysRevLett.111.023002](https://doi.org/10.1103/PhysRevLett.111.023002)

Electron-nuclear energy sharing in above threshold multiphoton dissociative ionization of H₂

J. Wu^{1,2}, M. Kunitski², M. Pitzer², F. Trinter², L. Ph. H. Schmidt², T. Jahnke², M. Magrakvelidze³, C. B. Madsen³, L. B. Madsen⁴, U. Thumm³, and R. Dörner^{2,†}

¹*State Key Laboratory of Precision Spectroscopy, East China Normal University, Shanghai 200062, China*

²*Institut für Kernphysik, Goethe Universität, Max-von-Laue-Strasse 1, D-60438 Frankfurt, Germany*

³*J. R. Macdonald Laboratory, Department of Physics, Kansas State University, Manhattan, Kansas 66506-2604, USA*

⁴*Department of Physics and Astronomy, Aarhus University, DK-8000 Aarhus C, Denmark*

Abstract

We report experimental observation of the energy sharing between electron and nuclei in above threshold multiphoton dissociative ionization of H₂ by strong laser fields. The absorbed photon energy is shared between the ejected electron and nuclei in a correlated fashion, resulting in multiple diagonal lines in their joint energy spectrum governed by the energy conservation of all fragment particles.

PACS number: 33.80.Rv, 42.65.Re, 42.50.Hz

[†] Electronic address: doerner@atom.uni-frankfurt.de

Deposition of the photon energy to atoms and molecules is the primary step of the interactions of radiation with matter. The details of this deposition process, in particular how the photon energy is distributed among the subsystems and various internal degrees of freedom, determine all photon-induced chemical and physical dynamics. For the interaction with a strong laser field, this question of energy deposition gets even richer since it is well established that energy of more photons than the minimal number required for ionization can be absorbed. For atoms in a strong field, this leads to discrete peaks in the photoelectron spectrum that are spaced by the photon energy and referred to as “above threshold ionization” (ATI) [1]. For molecules the vibrational, rotational and dissociative motions of the nuclei provide a sink for the photon energy in addition to the electrons. This has been observed in single-photon dissociative ionization of molecules exposed to synchrotron radiation [2-4], where the photon energy is shared by the freed electrons and the nuclear fragments.

For the molecular multiphoton case, rich ATI spectra of the freed electron [5-9], bond-softening-induced molecular dissociative ionization [10-15], and the imaging of internuclear distance using nuclear kinetic energy release spectra [16-19] have been reported. The correlation between the fragment ion and the electron energy has most recently been studied in numerical simulations for H_2^+ [20,21]. A non-trivial sharing of the absorbed photon energy between the electron and nuclei in multiphoton ionization of molecules was predicted and stimulated us to investigate this problem experimentally.

Here, we report the experimental observation of the energy sharing between the emitted electron and nuclei from above threshold multiphoton dissociative ionization of the simplest molecule H_2 by intense femtosecond laser pulses. Discrete numbers of absorbed photons can be identified by peaked diagonal lines in the joint energy spectrum (JES) of the coincidentally measured electron and nuclei [20]. Since there is no direct coupling between the nuclei and the laser field for homonuclear diatomic

molecules, the laser first couples to the electrons, and the electrons then couple to the nuclei. The energy taken by the nuclei therefore measures the correlation between the electrons and nuclei.

Figure 1 shows a much simplified schematics of the process. By absorbing multiple photons (blue vertical arrows), the H_2 molecule emits one electron and a nuclear wavepacket on the σ_g^+ (ground) state of H_2^+ is launched. It propagates on the σ_g^+ potential curve of H_2^+ . Part of this wavepacket already has sufficient energy to escape (direct pathway), while another part can be promoted to the dissociative σ_u^+ potential curve by resonant absorption of one additional photon (one-photon pathway). In the multiphoton picture, the sum of the kinetic energy of the proton (E_p), hydrogen atom (E_H), and electron (E_e) after the end of the laser pulse is given by

$$E_{\text{sum}} = E_e + E_p + E_H = n\omega - (I_{p0} + U_p). \quad (1)$$

Here I_{p0} and $U_p \sim 0.25E_L^2/\omega^2$ are respectively the field-free and the field-induced increase of the ionization potential of the neutral molecule in the laser field of amplitude E_L . We use atomic units throughout, unless indicated otherwise. To study this scenario and to see how the energy is shared between the electron and the nuclei in a given photoabsorption channel, the JES is measured.

We used ultraviolet (UV) light for our experimental study to be safely in the multiphoton ionization regime and to obtain a well spaced ATI spectrum. A linearly polarized UV pulse ($\lambda=390$ nm) was produced by frequency-doubling a near infrared (IR) pulse (35 fs, 780 nm, 8 kHz) in a 200- μm -thick β -barium borate (BBO) crystal, whose polarization could be varied to circular by a quarter waveplate. It was tightly focused onto a supersonic gas jet which was generated by expanding 2.0 bar H_2 through a 30 μm nozzle. A standard COLd Target Recoil Ion Momentum Spectroscopy (COLTRIMS) [22] was applied where the photo-ionization created ions and electrons were coincidentally detected by two time and position sensitive detectors. To estimate the temporal duration of the UV pulse inside the chamber, we collinearly

recombined the UV pulse and the near IR pulse with a dichroic mirror to drive the ionization of H_2 in the gas jet. By tracing the time-delay-dependent yield of H_2^+ as a cross-correlation of the recombined UV and near IR pulses, the temporal duration of the UV pulse inside the chamber was characterized to be 52 fs.

We determine the laser field intensity in the interaction region by making use of Eq. (1). We change the power of the laser pulse, measured with a power meter, and trace the change of E_{sum} as a function of laser power. As expected from Eq. (1), we find a linear dependence of E_{sum} on the laser power. From the slope of this linear dependence, we obtain U_p and hence the peak intensity in our focus to be 4.3×10^{13} W/cm² and 5.9×10^{13} W/cm² for linear and circular polarized UV pulses, respectively. Accordingly, the Keldysh parameter [23] was calculated to be $\gamma = 3.6$ and 4.2 well in the multiphoton ionization regime.

Figure 2(a) shows the measured electron-nuclear JES, i.e. E_e vs. E_N , of the above threshold multiphoton dissociative ionization of $\text{H}_2 + n\omega \rightarrow \text{H}^+ + \text{H} + e$ in a circularly polarized UV pulse. We will refer to this pathway as $\text{H}_2(1,0)$. The employment of a diffuse target jet and high vacuum conditions led to the extremely low event rate of ~ 0.1 electrons/laser shot for all ionization channels. This effectively reduced the false background counts to $< 7\%$ of the total counts. Only the H^+ and correlated electron e of the $\text{H}_2(1,0)$ channel were measured by the detectors in the experiment. We deduced the momentum of the neutral H based on the momentum conservation of the breaking system whose kinetic energy together with that of H^+ accounted for the total energy deposited to the nuclei, i.e. $E_N = E_p + E_H$. The corresponding energy spectra of the electron E_e , nuclei E_N , and their sum E_{sum} , are shown in Figs. 2(b), 2(c) and 2(d), respectively. The tilted lines in the electron-nuclear JES [20] evidently reflect the sharing of the absorbed photon energy, where the electron energy decreases with increasing of the nuclear energy for each, in compliance with energy conservation. Different from the single-photon dissociative ionization of molecules by synchrotron radiation [2-4], here we observe multiple JES lines in the strong field ionization of H_2

due to the absorption of multiple photons above the ionization threshold. For our laser intensity, more than six peaked JES lines are observed in Fig. 2(a). The excess photon energy over the ionization threshold is not only deposited to the outgoing electron, but also transferred to the heavy nuclei through their interactions with the electron.

To estimate how much photon energy is transferred to the nuclei, we appeal to a two-step classical model, i.e. the nuclei instantaneously acquire a kinetic energy of E_{N0} from their interaction with the outgoing electron in the first vertical ionization step. They then propagate on the H_2^+ potential curves, and dissociate to the continuum of the σ_g^+ (or σ_u^+) state, leading to the observable asymptotic nuclear energy E_N . To validate this two-step scenario, we numerically propagate the nuclear wavepacket by solving the time-dependent Schrödinger equation [24] in the subspace of the σ_g^+ and σ_u^+ states of H_2^+ , where the ionization from the ground state of H_2 to the σ_g^+ state of H_2^+ is simulated by employing either internuclear-distance-dependent molecular Ammosov-Delone-Krainov (ADK) rates [25] or a Franck-Condon vertical transition by replicating the H_2 initial vibrational wave function on the σ_g^+ ground state of H_2^+ . Dipole coupling between the σ_g^+ and σ_u^+ states is allowed during wavepacket propagation. The nuclear kinetic energy spectrum is calculated after a sufficiently long time propagation of the wavepacket after the end of the laser pulse. As shown in Fig. 3(a), the simulated distribution of E_N from the assumed initial Franck-Condon vertical ionization agrees much better with the experimental measurement than the prediction from the ADK-rate-weighted initial distribution. Figure 3(b) shows the Franck-Condon transition factors [26] for the transition $H_2 X^1\Sigma_g^+, v'=0 \rightarrow H_2^+ X^2\Sigma_g^+, v=0 \rightarrow 15$ as a function of the vibrational energy of E_v , whose vibrational energy is also shifted by 0.8 eV (dashed curve) accounting for the additional one photon absorption for a direct comparison with the nuclear kinetic energy release in Fig. 3(a). The vertical transition in the first ionization step indeed reproduces the pioneering observation of the ultrafast ionization of H_2 in the multiphoton regime [27]. It therefore confirms the validity of the above two-step scenario.

The σ_g^+ and σ_u^+ states of H_2^+ are degenerate at large internuclear distances where we define zero potential energy. Depending on whether the nuclear dissociation is direct or through the one-photon pathway, we have $E_{N0} = E_N - E_{g0}$ or $E_{N0} = E_N - E_{g0} - \omega$, respectively, where $E_{g0} = -1.9$ eV is the potential energy of the nuclei on the σ_g^+ curve of H_2^+ at the equilibrium internuclear distance of H_2 . As marked by the dashed line in Fig. 2(c), the nuclear energy spectrum can be distinguished into low and high energy regions, corresponding to the direct and one-photon dissociation pathways, respectively. As displayed in Fig. 2(a), the 1st ATI peak with low E_N is dominated by the direct dissociation, while the others with high E_N are mostly associated with the dissociation through the one-photon pathway. We will discuss the electron-nuclear energy sharing during the ionization for these two dissociation pathways and for the 1st and 2nd ATI peaks of the sum-energy spectrum.

Figure 3(c) plots the electron and nuclear energy spectra of the 1st ATI peak, where E_N shows a broad distribution compared to E_e which peaks at zero energy. This indicates that the nuclei take almost all the excess photon energy while the electron is most likely emitted with energies close to the ionization threshold. These energetic nuclei can therefore overcome the binding σ_g^+ potential well and directly dissociate. For the measured E_N centered at 0.38 eV in the continuum, we estimate that a total energy of $E_{N0} = 2.28$ eV is transferred to the nuclei during the strong-field multiphoton ionization. Since the electron transfers almost all the absorbed energy to the nuclei, this process is barely noticeable in a non-coincident integrated electron spectrum in Fig. 2(b), indicating the limitation of pure electron spectroscopic [5-7] for studying strong field ionization dynamics of molecules. As revealed in Figs. 2(a) and 2(d), however, it clearly shows up in the electron-nuclear JES and the sum-energy spectrum.

For the 2nd ATI peak dominated by the one-photon dissociation pathway, based on the measured E_N centered at 1.69 eV as shown in Fig. 3(d), we estimate the nuclei acquire only $E_{N0} = 0.41$ eV during the ionization. In this case the electron keeps most

of the energy absorbed from the laser, while the observable nuclear energy is mainly accumulated after the one-photon transition on the σ_u^+ potential curve. The nuclear dynamics are therefore strongly correlated with the electron. The amount of energy transferred to the nuclei during the ionization determines the succeeding dissociation dynamics of the molecular ion in strong laser fields.

Figure 4(a) shows the measured electron-nuclear JES of $H_2(1,0)$ in a linearly polarized UV pulse. By varying the polarization of the driving UV pulse from circular to linear, pronounced E_N - (and E_e -) dependent fine-structures appear in the resulting electron-nuclear JES lines. As shown in Fig. 4(b), the electron energy spectrum is correspondingly modulated with similar fine-structures as compared to the nuclear energy spectrum in Fig. 4(c). Interestingly, by considering the energies of all fragment particles, we can reconstruct a clear ATI spectrum [Fig. 4(d)] as observed for circularly polarized light, highlighting the correlated sharing of the photon energy by the ejected electron and nuclei. These results indicate that the fine-structures in the electron-nuclear JES most likely arise from the electron dynamics which depends strongly on the light polarization. Figure 4(b) shows that the fine-structure is most pronounced for the lower ATI peaks, and that the ATI spectrum is free from any plateau region. Hence, we conclude that the fine-structure is not due to any rescattering dynamics which could be present in the linearly polarized field (resulting in a plateau), but not for circular polarization.

To explain the origin of the fine-structure we refer to the pioneering experiments of Refs. [28-30], where non-coincident electron spectra were studied in the multiphoton above threshold ionization of atoms using linearly polarized ultrashort laser pulses. In those studies, the fine-structures were shown to come from Freeman resonances [28] of excited states during the multiphoton ionization. As in the current experiments the resonances could be switched off by going to circularly polarized pulses, because circular polarization leads to high angular momentum transfer to the excited electron which in turn diminishes the role of the resonances [31].

The fine-structures observed in our experiments differ from those in the electron-nuclear JES of the dissociative multiphoton ionization of H_2^+ as numerically predicted in Ref. [20]. There, the additional structures arise from the initial vibrational and electronic wavefunctions as revealed by the strong-field approximation analysis, and are insensitive to the light polarization since no intermediate state for resonance excitation was required. In contrast, the fine-structure in the current experiment is a hallmark of excited states, which is believed to be a more general phenomenon for multiphoton above threshold ionization of molecules [7]. To substantiate this claim, we point at other examples of fine-structure in molecular ATI spectra. One example is the details in the ATI spectrum recorded from strong-field ionization of laser-aligned CS_2 molecules [32]. Here, essentially anything but the role of excited states was ruled out to explain the fine-structure. Another example is found in the difference between the orientation-dependent yield for OCS in circularly [33,34] and linearly polarized fields [35]. The details of the yields differ due to the participation of excited states during the ionization dynamics in the linearly polarized field, and their minor role in circularly polarized fields.

In summary, we have investigated experimentally the correlated electron-nuclear dynamics in strong field multiphoton dissociative ionization of H_2 . The peaked multiple diagonal lines in the electron-nuclear joint electron spectrum evidently revealed the energy sharing between the emitted electron and nuclei. The electron-nuclear interaction during the multiphoton ionization may deposit considerable energy to the nuclei and therefore largely determines the succeeding dissociation dynamics. For linearly polarized ultrashort laser pulses, the non-coincident electron energy spectrum shows a rich structure dominated by Freeman resonances. The sum-energy of all fragments, however, recovers the same clear ATI spectrum as observed for circular light. Our results provide deeper insight into the strong-field multiphoton ionization of molecules, especially the fundamental mechanism of photon-energy deposition and sharing in the correlated motion of the electron and nuclei.

Acknowledgement: We thank Brett Esry for fruitful discussions. Support by the Deutsche Forschungsgemeinschaft, the Danish Natural Science Research Council, the ERC-StG (277767-TDMET), the US NSF, the Chemical Sciences, Geosciences, and Biosciences Division, Office of Basic Energy Sciences, Office of Science, and U.S. Department of Energy are acknowledged. J.W. acknowledges support by the Program for Professor of Special Appointment (Eastern Scholar) at Shanghai Institutions of Higher Learning and for New Century Excellent Talents in University (NCET-12-0177), and the “Shu Guang” project (12SG25).

References:

- [1] P. Agostini, F. Fabre, G. Mainfray, G. Petite, and N. K. Rahman, *Phys. Rev. Lett.* **42**, 1127 (1979).
- [2] A. Lafosse, M. Lebech, J. C. Brenot, P. M. Guyon, O. Jagutzki, L. Spielberger, M. Vervloet, J. C. Houver, and D. Dowek, *Phys. Rev. Lett.* **84**, 5987 (2000).
- [3] F. Martín, J. Fernández, T. Havermeier, L. Foucar, Th. Weber, K. Kreidi, M. Schöffler, L. Schmidt, T. Jahnke, O. Jagutzki, A. Czasch, E. P. Benis, T. Osipov, A. L. Landers, A. Belkacem, M. H. Prior, H. Schmidt-Böcking, C. L. Cocke, R. Dörner, *Science* **315**, 629 (2007).
- [4] T. Osipov, T. N. Rescigno, T. Weber, S. Miyabe, T. Jahnke, A. S. Alnaser, M. P. Hertlein, O. Jagutzki, L. P. H. Schmidt, M. Schöffler, L. Foucar, S. Schössler, T. Havermeier, M. Odenweller, S. Voss, B. Feinberg, A. L. Landers, M. H. Prior, R. Dörner, C. L. Cocke, and A. Belkacem, *J. Phys. B* **41**, 091001 (2008).
- [5] J. Verschuur, L. D. Noordam, and H. B. van Linden van den Heuvell, *Phys. Rev. A* **40**, 4383 (1989).
- [6] A. Zavriyev, P. H. Bucksbaum, H. G. Muller, and D. W. Schumacher, *Phys. Rev. A* **42**, 5500 (1990).
- [7] T. Wilbois and H. Helm, *Phys. Rev. A* **84**, 053407 (2011).
- [8] A. D. Bandrauk, S. Chelkowski, and I. Kawata, *Phys. Rev. A* **67**, 013407 (2003).
- [9] E. V. van der Zwan and M. Lein, *Phys. Rev. Lett.* **108**, 043004 (2012).
- [10] P. H. Bucksbaum, A. Zavriyev, H. G. Muller, and D. W. Schumacher, *Phys. Rev. Lett.* **64**, 1883 (1990).
- [11] A. Staudte, D. Pavičić, S. Chelkowski, D. Zeidler, M. Meckel, H. Niikura, M. Schöffler, S. Schössler, B. Ulrich, P. P. Rajeev, Th. Weber, T. Jahnke, D. M. Villeneuve, A. D. Bandrauk, C. L. Cocke, P. B. Corkum, and R. Dörner, *Phys. Rev. Lett.* **98**, 073003 (2007).
- [12] J. McKenna, M. Suresh, D. S. Murphy, W. A. Bryan, L. Peng, S. L. Stebbings, E. M. L. English, J. Wood, B. Srigengan, I. C. E. Turcu, J. L. Collier, J. F. McCann, W. R. Newell, and I. D. Williams, *J. Phys. B* **40**, 2607 (2007).
- [13] D. Ray, F. He, S. De, W. Cao, H. Mashiko, P. Ranitovic, K. P. Singh, I. Znakovskaya, U. Thumm, G. G. Paulus, M. F. Kling, I. V. Litvinyuk, and C. L. Cocke, *Phys. Rev. Lett.* **103**, 223201 (2009).
- [14] M. Magrakvelidze, F. He, T. Niederhausen, I. V. Litvinyuk, and U. Thumm, *Phys. Rev. A* **79**, 033410 (2009).
- [15] A. Picón, A. Jaroń-Becker, and A. Becker, *Phys. Rev. Lett.* **109**, 163002 (2012).

- [16] S. Chelkowski, P. B. Corkum, and A. D. Bandrauk, Phys. Rev. Lett. **82**, 3416 (1999).
- [17] Th. Ergler, A. Rudenko, B. Feuerstein, K. Zrost, C. D. Schröter, R. Moshhammer, and J. Ullrich, Phys. Rev. Lett. **97**, 193001 (2006).
- [18] I. A. Bocharova, H. Mashiko, M. Magrakvelidze, D. Ray, P. Ranitovic, C. L. Cocke, and I. V. Litvinyuk, Phys. Rev. A **77**, 053407 (2008).
- [19] K. J. Betsch, D.W. Pinkham, and R. R. Jones, Phys. Rev. Lett. **105**, 223002 (2010).
- [20] C. B. Madsen, F. Anis, L. B. Madsen, and B. D. Esry, Phys. Rev. Lett. **109**, 163003 (2012).
- [21] R. E. F. Silva, F. Catoire, P. Rivière, H. Bachau, and F. Martín, Phys. Rev. Lett. **110**, 113001 (2013).
- [22] R. Dörner, V. Mergel, O. Jagutzki, L. Spielberger, J. Ullrich, R. Moshhammer, and H. Schmidt-Böcking, Phys. Rep. **330**, 95 (2000).
- [23] L. V. Keldysh, Zh. Eksp. Teor. Fiz. **47**, 1945 (1964) [Sov. Phys. JETP **20**, 1307 (1965)].
- [24] J. Wu, M. Magrakvelidze, A. Vredenburg, L. Ph. H. Schmidt, T. Jahnke, A. Czasch, R. Dörner, and U. Thumm, Phys. Rev. Lett. **110**, 033005 (2013).
- [25] T. Niederhausen and U. Thumm, Phys. Rev. A **77**, 013407 (2008).
- [26] M. E. Wacks, J. Res. Nat. Bur. Stand. Sec. A Phys. Ch. **68A**, 631 (1964).
- [27] J. H. Posthumus, B. Fabre, C. Cornaggia, N. de Ruelle, and X. Urbain, Phys. Rev. Lett. **101**, 233004 (2008).
- [28] R. R. Freeman, P. H. Bucksbaum, H. Milchberg, S. Darack, D. Schumacher, and M. E. Geusic, Phys. Rev. Lett. **59**, 1092 (1987).
- [29] M. P. de Boer and H. G. Muller, Phys. Rev. Lett. **68**, 2747 (1992).
- [30] G. N. Gibson, R. R. Freeman, and T. J. McIlrath, Phys. Rev. Lett. **69**, 1904 (1992).
- [31] P. H. Bucksbaum, L. D. Van Woerkom, R. R. Freeman, and D. W. Schumacher, Phys. Rev. A **41**, 4119 (1990).
- [32] V. Kumarappan, L. Holmegaard, C. P. J. Martiny, C. B. Madsen, T. K. Kjeldsen, S. S. Viftrup, L. B. Madsen, and H. Stapelfeldt, Phys. Rev. Lett. **100**, 093006 (2008).
- [33] L. Holmegaard, J. L. Hansen, L. Kalhøj, S. L. Kragh, H. Stapelfeldt, F. Filsinger, J. Küpper, G. Meijer, D. Dimitrovski, M. Abu-samaha, C. P. J. Martiny and L. B. Madsen, Nat. Phys. **6**, 428 (2010).

[34] D. Dimitrovski, M. Abu-samaha, L. B. Madsen, F. Filsinger, G. Meijer, J. Küpper, L. Holmegaard, L. Kalhøj, J. H. Nielsen, and H. Stapelfeldt, *Phys. Rev. A* **83**, 023405 (2011).

[35] J. L. Hansen, L. Holmegaard, J. H. Nielsen, H. Stapelfeldt, D. Dimitrovski and L. B. Madsen, *J. Phys. B* **45**, 015101 (2012).

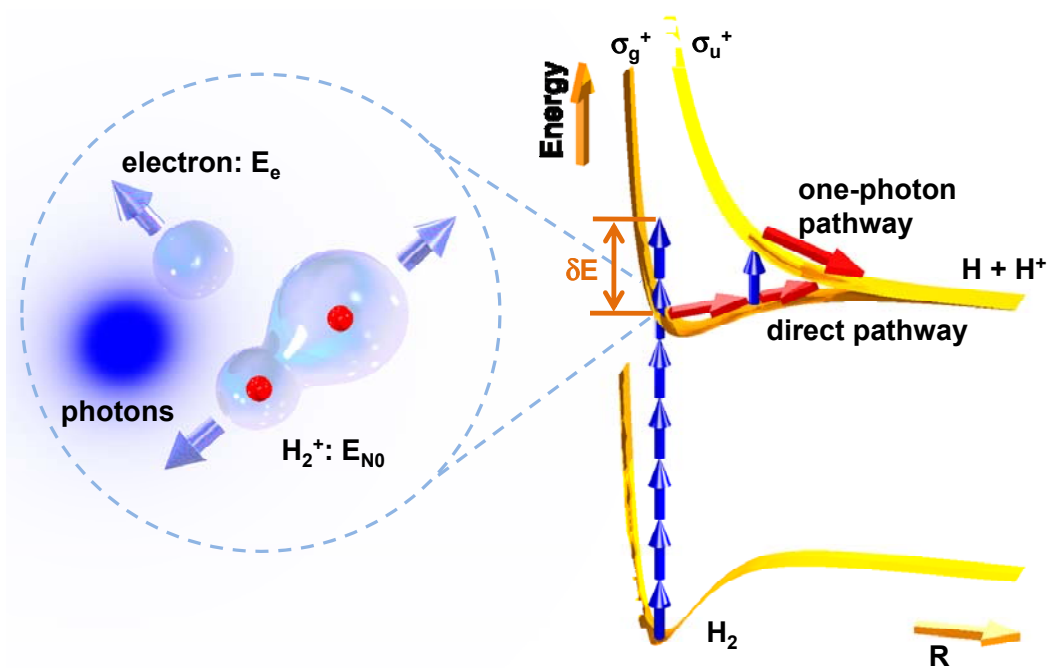


Figure 1 (Color online) Schematic illustration of the above threshold multiphoton dissociative ionization of H₂. The absorbed excess photon energy δE is deposited to the kinetic energies of the emitted electron (E_e) and the nuclei of H₂⁺ (E_{N0}), which may dissociate to H + H⁺ through either direct or one-photon pathways as indicated by the red arrows.

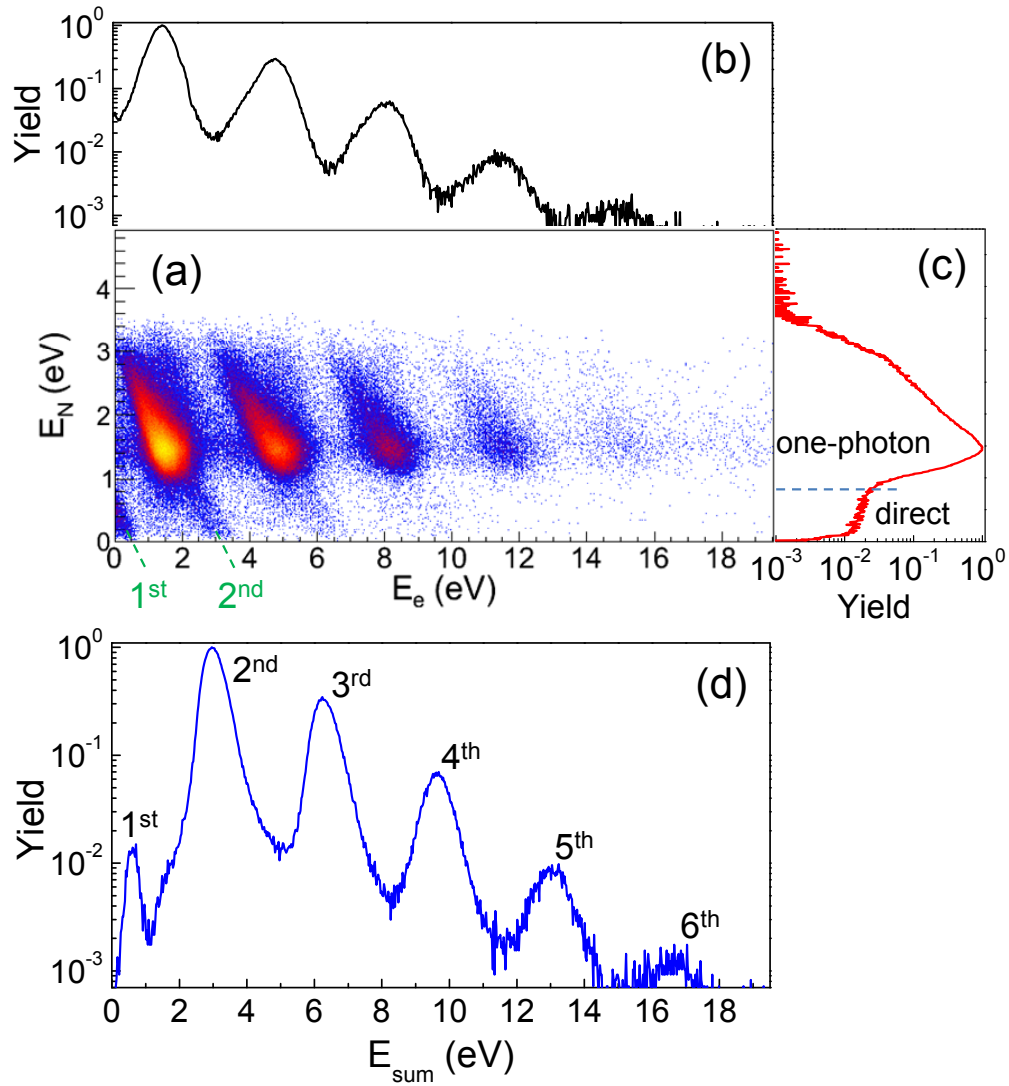


Figure 2 (Color online) (a) Electron-nuclear JES of the above threshold multiphoton dissociative ionization channel $H_2(1,0)$ in a circularly polarized UV pulse with a peak intensity of $I_0 = 4.3 \times 10^{13} \text{ W/cm}^2$. (b) Corresponding electron energy spectrum, (c) nuclear energy spectrum, and (d) electron-nuclear sum-energy spectrum. The numbers in the top of the peaks in (d) designate the different photon absorption channels above threshold. See Fig. 1 for an explanation of “direct” and “one-photon” in panel (c).

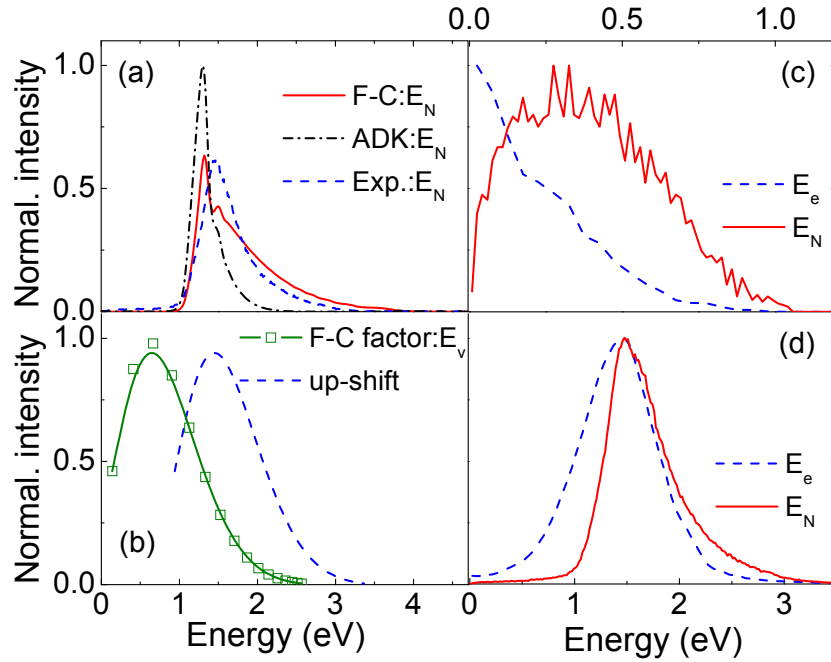


Figure 3 (Color online) (a) Kinetic energy distributions of $\text{H} + \text{H}^+$ measured in circularly polarized UV pulses and quantum simulated by assuming a Franck-Condon or ADK transition rate from H_2 to H_2^+ . (b) Franck-Condon factors. Electron and nuclear energy spectra of the (c) 1st and (d) 2nd sum-energy ATI peaks of $\text{H}_2(1,0)$ produced in a circularly polarized UV pulse.

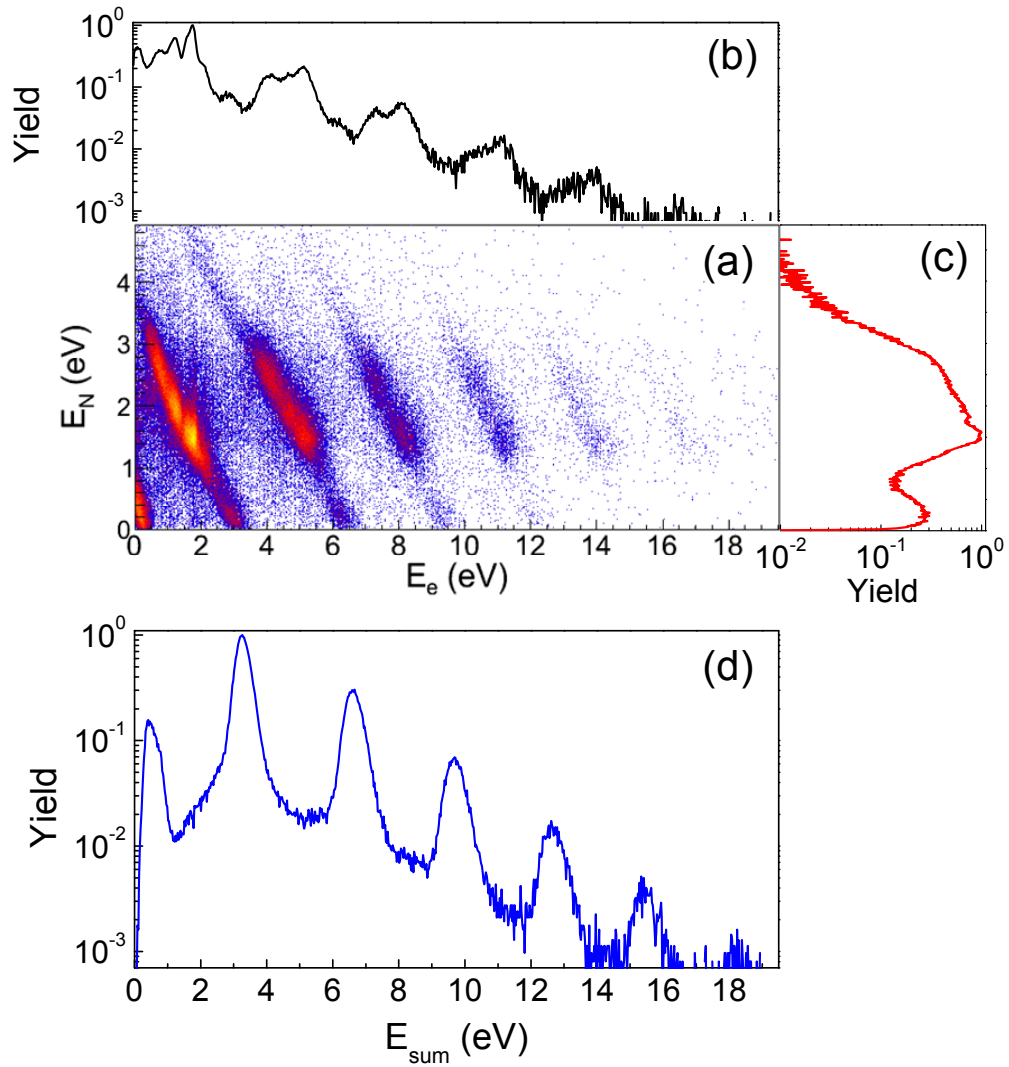


Figure 4 (Color online) Same as Fig. 2 but for a linearly polarized UV pulse with a peak intensity of $I_0 = 5.9 \times 10^{13} \text{ W/cm}^2$.